Tetrahedron 72 (2016) 2072–2083

Contents lists available at ScienceDirect

Tetrahedron

journal homepage: www.elsevier.com/locate/tet

Conformations, equilibrium thermodynamics and rotational barriers of secondary thiobenzanilides

Ján Kozic [a,*], Zdeněk Novák [a], Václav Římal [b], Václav Profant [c], Jiří Kuneš [a], Jarmila Vinšová [a]

[a] Department of Inorganic and Organic Chemistry, Faculty of Pharmacy in Hradec Králové, Charles University in Prague, Heyrovského 1203, 500 05 Hradec Králové, Czech Republic
[b] Department of Low Temperature Physics, Faculty of Mathematics and Physics, Charles University in Prague, V Holešovičkách 2, 180 00 Prague 8, Czech Republic
[c] Institute of Physics, Faculty of Mathematics and Physics, Charles University in Prague, Ke Karlovu 5, 121 16 Prague 2, Czech Republic

ARTICLE INFO

Article history:
Received 14 November 2015
Received in revised form 7 February 2016
Accepted 15 February 2016
Available online 27 February 2016

Keywords:
Thiobenzanilide
E, *Z*-conformer
Axial chirality
Rotational barrier

ABSTRACT

The article deals with conformational behaviour of 2-methoxy-2′-hydroxythiobenzanilides. The CS-NH group of these compounds preferentially adopts the *Z*-conformation. Entropy favours the *Z*-conformer over the *E*-conformer, whereas enthalpy slightly favours the *E*-conformer over the *Z*-conformer. The rotational barrier about the CS-NH bond was determined to be (81.5±0.4) kJ/mol. No significant rotational barrier was found on the Ar–CS and Ar–NH bonds. All experimental outcomes are compared with the results of quantum-chemical calculations.

1. Introduction

Benzanilides are a group of compounds which can possess two stereochemically striking features: *E*, *Z*-conformation on the CO–N bond and/or axial chirality on the Ar–CO/Ar–N axis. During the last century there has been a great deal of interest into the stereochemistry of the amide group because of its significance for protein conformation. Nowadays, it is well-known that secondary benzanilides preferentially adopt the *Z*-conformation whereas tertiary benzanilides generally prefer the *E*-conformation on CO–N bond (Fig. 1). The preferred conformation is determined by substitution on the nitrogen atom of the amide group and by *ortho*-substitution on the aromatic rings.[1,2]

On the other hand, the axial chirality of benzanilides, which arises from the more or less perpendicular arrangement of the amide group to the plane of the aromatic ring and restricted rotation around the bond of the aromatic ring to the amide group, has been a subject of intense study for the last two decades. Today, the atropisomerism of tertiary benzamides is well-known and has been exploited in different ways. It was shown that the conformation of the Ar–CO bond can exert a powerful kinetic control over the formation of a nearby stereogenic centre—amide group as a chiral auxiliary.[3–6] Further, it was revealed that the adjacent stereogenic centre can thermodynamically govern the conformation of the Ar–CO bond. This was exploited for the transmission of stereochemical information between two remote stereogenic centers in the molecule–remote asymmetric induction.[7,8] Finally, enantiomerically pure atropisomeric tertiary benzamides were prepared and successfully used as chiral ligands in Pd-catalysed allylic substitution reactions. In this case the stereochemical information of conformation of the Ar–CO bond was transmitted into another molecule. This is the first use of a nonbiaryl atropisomer as a chiral ligand.[9] Axial chirality of anilides is also well-known and was studied for example in regard to the prochiral auxiliary approach to asymmetric synthesis.[2]

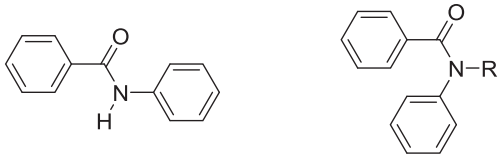

Z-conformer *E*-conformer

Fig. 1. Preferred conformation of the amide group of benzanilides, R=alkyl.

* Corresponding author. Fax: +420 49 5514166; e-mail addresses: jan.kozic.ml@gmail.com, jan.kozic@faf.cuni.cz (J. Kozic).

http://dx.doi.org/10.1016/j.tet.2016.02.035
0040-4020/

Conversely, thiobenzanilides are stereochemically much less explored counterparts of benzanilides, although it is well-known that the thioamide bond has a greater rotational barrier than the amide bond, and the sulfur atom of the thioamide group is bulkier than the oxygen atom of the amide group. In the literature there are only a few articles dealing with axial chirality of thiobenzanilides,[10,11] and to the best of our knowledge, there is only one article concerning axial chirality of secondary thiobenzanilides.[12]

Recently, we have prepared a series of antimycobacterially active derivatives of 2-methoxy-2′-hydroxythiobenzanilide. For all of the prepared thiobenzanilides it was possible to observe two series of NMR resonance signals in ^{1}H and ^{13}C NMR spectrum measured at 25 °C in DMSO-d_6.[13] Therefore, we initiated a study to clarify this phenomenon and to investigate the stereochemical behaviour of derivatives of 2-methoxy-2′-hydroxythiobenzanilide.

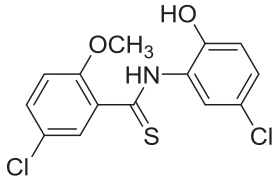

Fig. 2. Compound **1**.

2. Results and discussion

2.1. *E*, *Z*-conformation of 2-methoxy-2′-hydroxythiobenzanilides

At the outset of the study, the cause of the presence of two series of NMR resonance signals in the ^{1}H and ^{13}C NMR spectrum of 2-methoxy-2′-hydroxythiobenzanilides was investigated. First of all, ^{1}H NMR spectrum of compound **1** (Fig. 2) was recorded in DMSO-d_6 at temperatures ranging from 30 to 120 °C (Fig. 3). Gradual coalescence of both series of resonance signals was observed with increasing temperature and finally at 90–100 °C the two series merged into one series of broad resonance signals. When the sample was cooled down, the two series were restored. From these results it was concluded that the two series of NMR resonance signals belong to two conformers of compound **1**. These conformers manifested themselves spectroscopically in the NMR spectrum due to slow rotation on the NMR timescale, but could not be isolated due to fast rotation on the laboratory timescale.

The assignment of conformers was performed by a NOESY NMR experiment. The proton of the NH group of the major conformer has an equally strong correlation with H6 and H6′, whereas the proton of the NH group of the minor conformer correlates only with H6′ (Figs. 4 and 5).

From this observation, it was concluded that the two conformers are *E*, *Z*-conformers around the CS–NH bond. The more populated

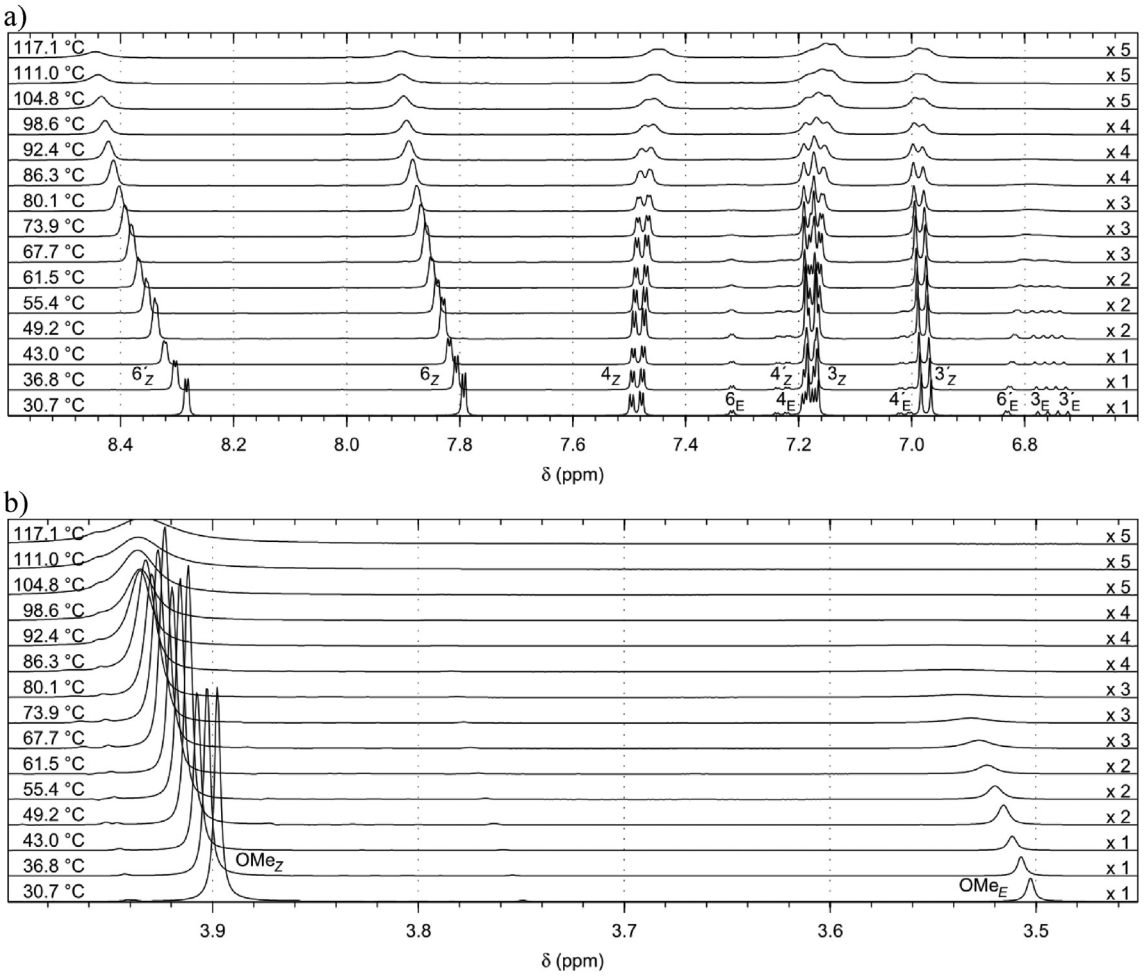

Fig. 3. The impact of increasing temperature on the chemical shifts and line-shapes in the a) aromatic and b) aliphatic part of ^{1}H NMR spectrum of compound 1 (500 MHz, DMSO-d_6, 30–120 °C). For better clarity of broadening resonances, the vertical scales are changing with increasing temperature (indicated on the right). Assignment of the resonances for both conformers is indicated.

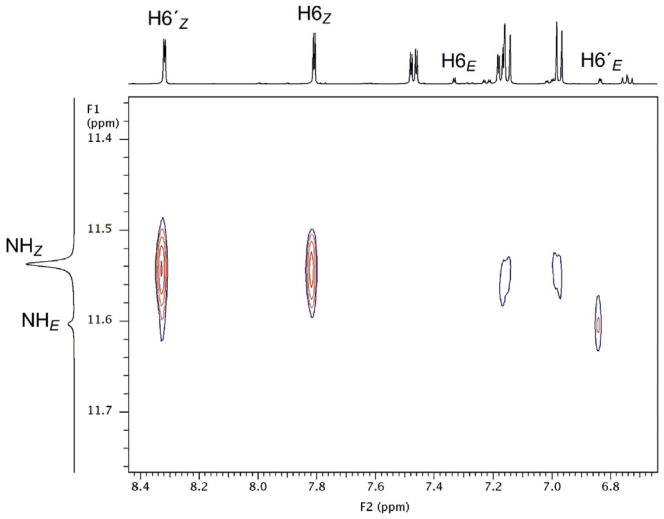

Fig. 4. The partial NOESY spectrum (500 MHz, DMSO-d_6, 25 °C, mixing time 700 ms) of compound **1**.

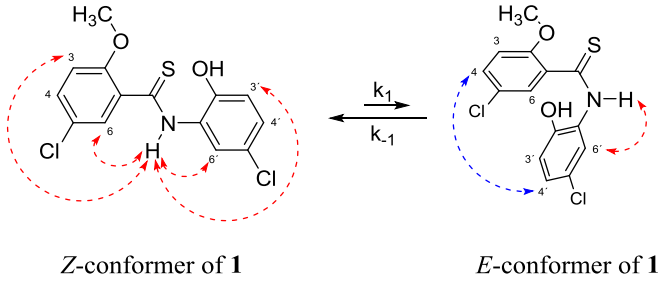

Fig. 5. *Z* and *E*-conformers of compound **1** around the CS–NH bond with the NOESY correlations (red dashed arrows) and the 1D NOE correlation (blue dashed arrow).

conformer is the *Z*-conformer and the less populated one is the *E*-conformer (Fig. 5). The supporting evidence was provided by a 1D NOE experiment, the polarization transfer from H4 to H4′ was observed only for the minor conformer (*E*) (Figs. 5 and 6).

The relationship between the solvent and the ratio of *E*, *Z*-conformers was also investigated (Table 1). However, no apparent relationship between solvent properties (boiling point, density, viscosity and relative permittivity) and *E*, *Z*-conformational ratio was revealed.

Table 1
Z/*E* ratio of **1** in different solvents at 25 °C

Solvent	*Z*/*E* (%)[a]
$CDCl_3$	90:10
Acetone-d_6	97:3
CD_3OD	93:7
DMSO-d_6	86:14
DMF-d_7	94:6
Pyridine-d_5	92:8
THF-d_8	95:5

[a] Determined by ^{1}H NMR at 25 °C, without calibration curve.

In the next part of the study, we focused on the structural features, which are responsible for the ratios *E*, *Z*-conformers of compound **1**. The presence of the sulfur atom of the thioamide group has a crucial role. For the amide analogue of compound **1** it was not possible to observe an *E*, *Z*-equilibrium in the NMR spectrum. To examine the importance of *ortho* substituents on aromatic rings, the series of compounds with modification at the *ortho* position were synthesized (Fig. 7).

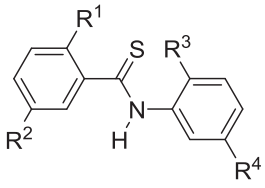

	R^1	R^2	R^3	R^4
1	OCH_3	Cl	OH	Cl
2	H	Cl	OH	Cl
3	OCH_3	Cl	H	Cl
4	Cl	Cl	OH	Cl
5	OCH_3	Cl	CH_3	Cl
6	OCH_3	H	OH	H
7	CH_2CH_3	H	OH	Cl
8	OCH_3	Cl	CH_2CH_3	H

Fig. 7. Modifications of compound **1**.

Initially, a compound without methoxy (**2**) or hydroxy (**3**) group was prepared. For both of these derivatives only one series of NMR resonance signals was observed (Table 2). Thereafter, the *ortho* substituent was replaced by a substituent of the same size and without hydrogen bond acceptor/donor ability. The aim of this modification was to investigate whether the steric properties or hydrogen bonding ability of *ortho* substituents are responsible for the observation of *E*, *Z*-conformers. The OCH_3 group was replaced by a Cl atom (**4**) and OH group by CH_3 (**5**). In both cases, *E*, *Z*-conformers were observed and their ratio was more or less the same as for compound **1** (Table 2). From these observations it was

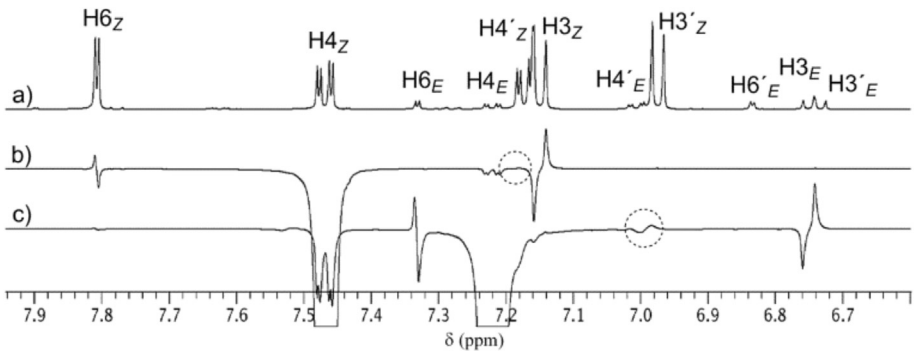

Fig. 6. 1D NOE spectrum of compound **1**. a) ^{1}H NMR spectrum, b) 1D NOE with irradiated signal H4 of *Z*-conformer, c) 1D NOE with irradiated signal H4 of *E*-conformer. Dotted circles represent regions of H4′of the two conformers (500 MHz, DMSO-d_6, 25 °C, 8000 transients, mixing time 200 ms).

Table 2
Z/*E* ratio of thioamides **1**–**8** in DMSO-d_6 at 25 °C

Thioamide	*Z*/*E* (%)[a]
1	86:14
2	—[b]
3	—[b]
4	90:10
5	88:12
6	88:12
7	95:5
8	95:5

[a] Estimated by ^{1}H NMR at 25 °C, without calibration curve.
[b] *E*, *Z*-equilibrium was not observed.

concluded that the main property of the *ortho* substituents responsible for the observation of *E*, *Z*-conformers is their size. No intramolecular hydrogen bonds are formed and it is the steric hindrance which causes the *E*, Z-conformers visible in the NMR spectra. Substituents at another position in the aromatic rings have no impact on the *E*, *Z*-conformers (**6**) (Table 2).

2.2. NMR analysis of the equilibrium and dynamics of 1

Finally, we focused on determination of the energy difference ΔG between the *E* and *Z*-conformers of compound **1** and their barrier of interconversion. This task was solved by means of VT (variable temperature) NMR. Fig. 3 shows a series of ^{1}H NMR spectra acquired at temperature ranging from 30.7 °C to 117.1 °C with a step of approximately six degrees. From the line-shape analysis of the spectra, the enthalpy change ΔH=(−3.1±1.3) kJ/mol and entropy change ΔS=(−26.9±3.6) J/mol/K for the *Z* to *E* transition was determined by the fit of the van't Hoff equation (Fig. 8). The weak enthalpy decrease can be assigned to a stabilization effect of π-π stacking interaction present in the *E*-conformer. The entropy penalty of the *E*-conformer can be attributed to the more constrained conformational space of this conformer relative to the *Z*-conformer. Based on the above mentioned values, ΔG of transition from *Z*-conformer of **1** to *E*-conformer of **1** was calculated to be (+4.9±0.3) kJ/mol at 25 °C. This value means that at 25 °C the compound **1** is a mixture of 88% *Z*-conformer and 12% *E*-conformer. This conformer distribution is slightly different from the one obtained by integration of NMR signals (86% *Z*-conformer and 14% *E*-conformer).

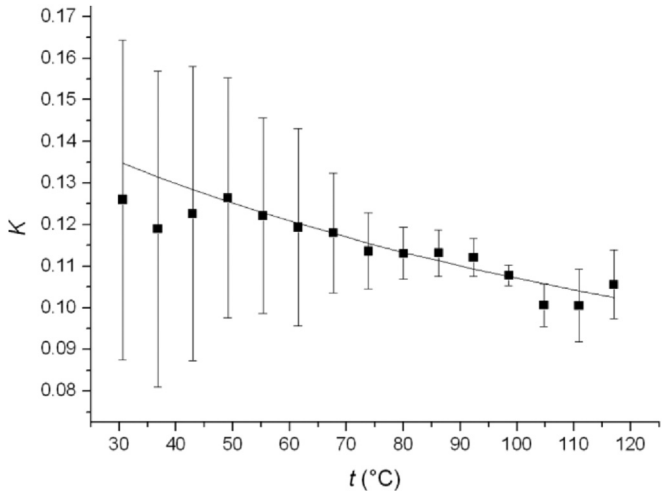

Fig. 8. Temperature dependence of equilibrium constant *K* for *Z* to *E* transition of **1**. Solid line: van't Hoff fit.

The activation enthalpy $\Delta H^{\dagger}$=(+77.7±1.7) kJ/mol and the activation entropy $\Delta S^{\dagger}$=(−12.5±4.6) J/mol/K were also estimated from the Eyring fit of the exchange rates for the *Z* to *E* transition of compound **1** (Fig. 9). The rotational barrier $\Delta G^{\dagger}$ of transition of *Z*-conformer of **1** to *E*-conformer of **1** was determined to be (81.5±0.4) kJ/mol at 25 °C. The enthalpy of activation is rather high and we connect it to the disruption of the partial double character of the C–N thioamide bond during rotation. This is in accordance with the general opinion. The activation entropy is approximately half of the entropy change of the whole conformational change, so from an entropy point of view, the transition state is just on the midway between the two conformers.

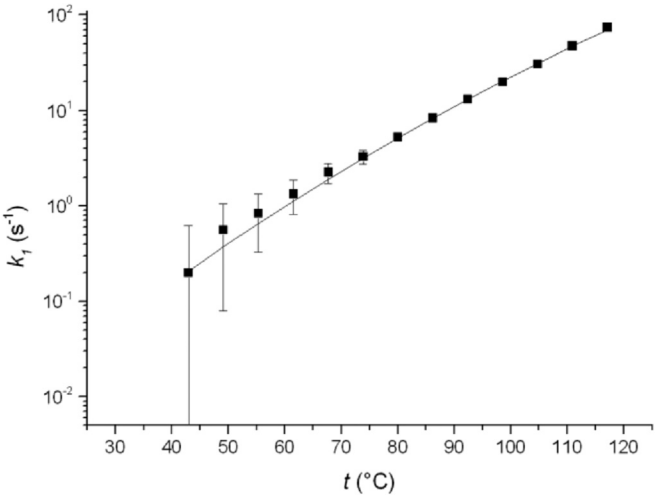

Fig. 9. Temperature dependence of the rate constant k_1 for *Z* to *E* transition of compound **1**. Solid line: Eyring fit.

Based on the line-shape analysis of the spectra it was found that k_1 (Fig. 5) is 0.033 s^{-1} and k_{-1} (Fig. 5) is 0.24 s^{-1} at 25 °C. This means that the half-life at 25 °C is 21.3 s for *Z*-conformer of **1** and 2.9 s for *E*-conformer of **1**. This makes the conformers visible on NMR time scale, but makes impossible to isolate them on laboratory time scale.

2.3. DFT calculations of the equilibrium and dynamics of 1

To obtain independent verification of the above experimental results, quantum-chemical calculations of compound **1** were performed. Experimental study was carried out in solution, DMSO in our case, the influence of which cannot be precisely mimicked in computation. The best results were obtained using a combined solvent model consisting of one explicit DMSO molecule H-bonded to the thioamide hydrogen and an implicit polarized continuum model COSMO for the surrounding environment. The initial step of the calculation was the determination of possible conformers of **1**.

The thioamide group can adopt either *Z* or *E*-conformations, nevertheless, the relative orientation of lateral phenyl groups to the plane of the thioamide group can vary. Therefore, the potential energy scans across dihedral angles α, β, and ω (α=ϕ_{C2C1CN}; β=$\phi_{CNC1'C2'}$; ω=$\phi_{C1CNC1'}$) were performed to elucidate conformers which have to be taken into account (DFT/B3LYP/6-31G/cpcm(DMSO) level of theory, 5° step). The scans identified four minima for both angles α and β (roughly $\alpha\in\{-130°, -70°, 50°, 110°\}$; $\beta\in\{-115°, -55°, 65°, 125°\}$) and confirmed two main conformations of the thioamide bond ($\omega\in\{0°, 180°\}$). This led to the preparation of 32 starting models (16 for each conformation of

thioamide bond) for geometry optimization performed at DFT/B3LYP/6-311++G**/cpcm(DMSO) level. During the optimization, some of the models converged to the same energy and geometry, which resulted in the final number of 8 conformers for the *E*-conformer and 6 conformers for the *Z*-conformer. The structural parameters of all optimized conformers are shown in Table 3 which also contains their calculated energies (expressed as differences related to the lowest energy conformer) and relative proportions based on the Boltzmann distribution at 25 °C. Three different thermodynamic energies are shown: the pure energy (ΔE), energy corrected for zero point vibrational energy (ΔE_0), and enthalpy (ΔE_H). The most suitable for the comparison with the experimental values is the latter one, however, conformer proportions remain similar in all cases.

structures of the *E*/*Z* interconversion. The first energy maximum of the rotation (TS_1) is at dihedral angle $\omega \sim -95°$, the second one (TS_2) at the dihedral angle $\omega \sim 95°$. After the re-optimization of both transition states on the higher level of theory (DFT/B3LYP/6-311++G**/cpcm(DMSO)) and calculation of thermodynamic properties, the energy difference between the most stable conformation of the CS–NH bond (Z6-conformer in Table 3) and the transition state of interconversion was calculated as $\Delta E_H^{\ddagger}$=82.6 kJ/mol for TS_1 and $\Delta E_H^{\ddagger}$=79.0 kJ/mol for TS_2. These values relatively well correspond to the experimentally determined activation energy $G_{25\,°C}^{\ddagger}$=(81.5±0.4) kJ/mol which lies right between them.

The further improvement of accuracy of activation energy computations would require more accurate covering of effects of solvation what is rather difficult.

Table 3
Structural and thermodynamic parameters of the optimized conformers of **1**

Conformer	Dihedral angle (°)			Distance from the amide H (Å)							Energy (kJ/mol)			n (%)		
	α	β	ω	H6	H6′	H3	H3′	OCH_3			ΔE	ΔE_0	ΔE_H	ΔE	ΔE_0	ΔE_H
E1	−119	66	6	3.69	2.69	6.58	5.26	6.05	6.34	6.58	12.61	12.97	12.58	0.1	0.1	0.1
E2	−101	−121	6	3.92	3.42	6.46	4.84	5.71	6.09	6.32	6.05	6.94	6.48	1.6	1.2	1.4
E3	−64	131	−7	4.41	3.48	6.17	4.78	4.98	5.49	5.78	3.54	3.75	3.48	4.5	4.3	4.6
E4	−74	−74	−7	4.34	2.89	6.19	5.18	5.08	5.54	5.86	5.15	5.36	4.98	2.4	2.3	2.5
E5	72	72	8	4.36	2.88	6.17	5.19	5.04	5.51	5.83	5.17	5.61	5.05	2.4	2.0	2.4
E6	65	−131	7	4.40	3.48	6.17	4.79	4.99	5.5	5.79	4.04	4.94	4.35	3.7	2.7	3.2
E7	98	114	−4	3.98	3.34	6.42	4.91	5.63	6.02	6.26	5.15	5.76	5.44	2.4	1.9	2.1
E8	118	−68	−6	3.71	2.73	6.57	5.25	6.03	6.32	6.57	12.40	12.90	12.41	0.1	0.1	0.1
													sum	**17.2**	**14.6**	**16.5**
Z1	−81	−121	−179	3.60	3.43	4.89	4.83	4.42	4.61	5.17	1.37	1.25	1.22	10.9	11.8	11.4
Z2	−75	−85	−177	3.67	2.93	4.89	5.16	4.38	4.56	5.13	1.41	1.37	1.34	10.7	11.3	10.9
Z3	−75	90	178	3.69	3.06	4.87	5.09	4.36	4.53	5.10	0.00	0.18	0.10	18.9	18.2	18.0
Z4	87	107	178	3.47	3.28	5.00	4.95	4.61	4.82	5.33	0.81	0.62	0.58	13.6	15.3	14.8
Z5	69	82	177	3.79	2.87	4.82	5.19	4.27	4.39	5.00	1.59	1.85	1.64	10.0	9.3	9.7
Z6	75	−93	−178	3.67	3.10	4.88	5.07	4.41	4.57	5.13	0.03	0.00	0.00	18.7	19.6	18.7
													sum	**82.8**	**85.4**	**83.5**

Values of the dihedral angles in Table 3 indicate that the mutual orientation of the phenyl groups affects the precise value of the dihedral angle ω. This is more pronounced in the case of the *E*-conformer which manifests a noticeable degree of nonplanarity between −7 and +8°. In accordance with experimental observations, none of the calculated conformers manifests the possibility of forming an intramolecular hydrogen bond. Most stable conformers—Z6 and E3—are shown in Fig. 10a, b.

Based on the energy difference between the *E* and *Z*-conformers, the *E*/*Z* ratio can be determined. The calculated energy difference between the *Z* and *E*-conformer of **1** is ΔE_H=−4.1 kJ/mol (obtained as the difference of the weighted averages of the *E* and *Z*-conformers energies), which is close to the free energy difference obtained from VT NMR line-shape analysis, $\Delta G_{25\,°C}$=(−4.9±0.3) kJ/mol. As shown in Table 3, based on ΔE_H values, compound **1** should be composed from 16% of the *E*-conformers and 84% of the *Z*-conformers. This is in very good accordance with the experimental results obtained from the ^{1}H NMR spectra (see Table 2 and text).

A computational study aimed at determining the rotational barrier of interconversion of *E*, *Z*-conformers of **1** was also undertaken. The simulation of rotation about the CS–NH bond was done for the most stable conformers of each orientation of the thioamide bond (E3 and Z6) with 2.5° step at DFT/B3LYP/6-31G**/cpcm(DMSO) level. For both conformers, simulations provided almost identical energy profiles with two relatively broad local energy minima. The first one ($\omega \sim 180°$) corresponds to the *Z*-conformation on the thioamide bond and the second one, which is dual ($\omega \sim 8°$, $-8°$), belongs to the *E*-conformation on the thioamide bond (Fig. 10c). There were also revealed two energy maxima which represents the transition

2.4. Aryl groups conformations

The next part of this study was focused on the conformation of compound **1** around the Ar–CS and Ar–NH bonds (dihedral angles α and β, respectively). In the NOESY spectrum (Fig. 4), there are correlations of the hydrogen atom of the CSNH group with H6, H6′, H3 and H3′ hydrogen atoms. Thus, it was concluded that either the rotation along these bonds is more or less free, or the rotation is hindered and the aromatic rings are out of the plane of the thioamide group. To distinguish between these two possibilities, properties of noncoplanar conformation were exploited. In this case, if the rotations about the Ar–CS/Ar–NH bonds were sufficiently hindered, the molecule would exhibit axial chirality. To prove possible axial chirality, a group containing geminal hydrogens (ethyl group) was introduced into the *ortho* position. Compounds **7** and **8** were prepared and their NMR spectra were recorded at 25 °C as well as at −80 °C in THF-d_8, but no separate diastereotopic signal for the methylene group was observed. The same results were obtained in the case of NMR spectra recorded in $CDCl_3$, DMF-d_7, and CD_3CN. From these results it was concluded that the rotations about the Ar–CS/Ar–NH bonds are more or less free at 25 °C and the hypothesis of axial chirality of **1** was rejected.

To independently support experimental findings the computational study of rotation around Ar–CS and Ar–NH bonds was carried out. Several rotational scans at DFT/B3LYP/6-31G**/cpcm(DMSO) level were performed for both *Z* and *E*-conformers to cover all possible spatial arrangements of both phenyl groups. In the case of the *Z*-conformer, the rotation around the Ar–CS bond was computed for four initial conformers (Z1, Z3, Z4 and Z6)

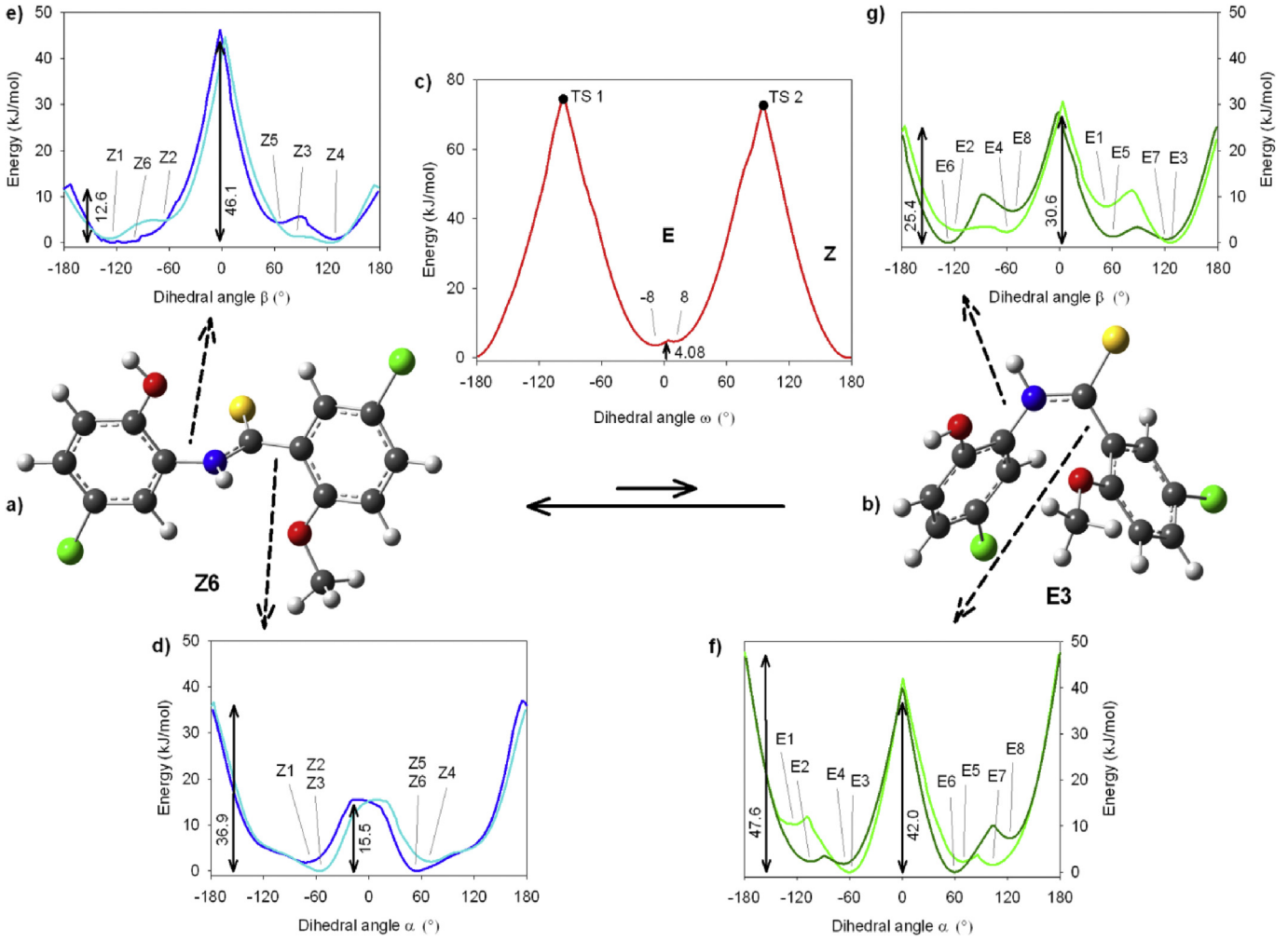

Fig. 10. a), b) Most stable conformer of *Z* (a) and *E* (b) -conformer of 1 as determined by QM calculations (explicit solvent molecules not shown). c) Energy profile of rotation around CS–NH bond (dihedral angle ω) of conformer Z6 with marked transition states and energy minima. d), e) Energy profile of rotation around Ar–CS bond (d) and Ar–NH bond (e) of *Z*-conformer, calculated for Z3 and Z6 conformer (light and dark blue line, respectively); minima corresponding to the particular conformers are labeled. f), g) Energy profile of rotation around Ar–CS bond (f) and Ar–NH bond (g) of *E*-conformer, calculated for E3 and E6 conformer (light and dark green line, respectively); minima corresponding to the particular conformers are labeled. All conformers are labeled according to Table 3.

differing in the value of the β angle. The obtained energy profiles of the Z1 and Z4 conformers were similar to those of the Z6 and Z3 conformers, respectively. The latter two profiles are shown in Fig. 10d. There can be observed several local minima around $\alpha \sim \pm 60°$, which correspond to individual *Z*-conformers, and two maxima. The first maximum is located at $\alpha \sim 180°$ and forms a barrier for free 360° rotation (ΔE=36.9 kJ/mol, $k=2.1 \cdot 10^6$ s^{-1} at 25 °C). The second rather low maximum (ΔE=15.5 kJ/mol) at $\alpha \sim 0°$ can be easily exceeded ($k=1.2 \cdot 10^{10}$ s^{-1} at 25 °C) which means that *Z*-conformer of compound **1** can almost freely change the value of its dihedral angle α in the interval between −150 and 150°.

The rotation scan around the Ar–NH bond of the *Z*-conformer was performed for conformers Z3 and Z6 representing the negative and positive value of α angle, respectively (see Table 3). In the obtained energy profiles (Fig. 10e) six local energy minima were identified corresponding to all *Z*-conformers. There are also two maxima located at $\beta \sim 0°$ and $\beta \sim 180°$, the second one being negligible (ΔE=12.6 kJ/mol, $k=3.8 \cdot 10^{10}$ s^{-1} at 25 °C). Therefore, only the first maximum (ΔE=46.1 kJ/mol, $k=5.1 \cdot 10^4$ s^{-1} at 25 °C) prevents a free 360° rotation around the Ar–NH bond. Thus, both α and β dihedral angles in the *Z*-conformer may easily change their value within (at least) 300° wide interval which can explain the missing evidence for axial chirality in compounds **7** and **8**. The energy barriers at $\alpha \sim 180°$ and $\beta \sim 0°$ are caused by electrostatic repulsion between the free electron pairs of sulfur and oxygen from either the methoxy or hydroxy group. The repulsion causes a deflection of the sulfur atom from the planar arrangement of the thioamide group and increment of the energy. As the distance between sulfur and oxygen is shorter in the case of $\beta \sim 0°$, i.e., hydroxylated phenyl group, the repulsion and therefore also the energy barrier is higher.

Similar rotational studies were performed for the *E*-conformer. The rotation around the Ar–CS bond was computed for four initial conformers (E3, E4, E5 and E6) representing main values of the β angle. The obtained energy profiles of the E5 and E4 conformers were similar to those of E3 and E6 conformers, respectively. The latter two profiles are shown in Fig. 10f. There were eight local minima observed, which correspond to all individual *E*-conformers, and two maxima. The first maximum is located at $\alpha \sim 180°$ and forms a barrier for free 360° rotation with ΔE=47.6 kJ/mol ($k=2.8 \cdot 10^4$ s^{-1} at 25 °C). The second maximum at $\alpha \sim 0°$, nearly three times higher compared to the *Z*-conformer (Fig. 10d), forms a second barrier with ΔE=42.0 kJ/mol ($k=2.7 \cdot 10^5$ s^{-1} at 25 °C) hampering the free phenyl rotation.

The rotation scan around the Ar–NH bond of the *E*-conformer was also performed for four initial conformers (E2, E3, E6 and E7) representing the main values of the α angle. The obtained energy

profiles of the E2 and E7 conformers were similar to those of E3 and E6 conformers, respectively. In the obtained rotational energy profiles of the latter two conformers (Fig. 10g) eight local energetic minima were identified corresponding to all *E*-conformers. There are also two energy maxima located at $\beta\sim0^\circ$ (ΔE=30.6 kJ/mol; $k=2.7\cdot10^7$ s^{-1} at 25 °C) and $\beta\sim180^\circ$ (ΔE=25.4 kJ/mol; $k=2.2\cdot10^8$ s^{-1} at 25 °C) both forming barriers to a free 360° rotation around the Ar–NH bond. In the case of the *E*-conformer, energy barriers originate mostly from the π-π stacking interaction and the intrinsic steric reasons, i.e., the proximity of both phenyl groups and mutual hindering during their rotation. This is stressed in the case of $\alpha\sim0^\circ$ or $\beta\sim180^\circ$ when methoxy and hydroxy groups, respectively, point towards the adjacent phenyl. The electrostatic repulsion between free electron pairs also takes place, primarily in the case of $\alpha\sim180^\circ$. In summary, calculations indicate that the rotational motions of phenyl groups in the *E*-conformer are more hindered compared to the *Z*-conformer, which leads to an entropy loss. This is in accordance with the finding of the line-shape analysis of the VT NMR spectra.

1D NOE buildup experiments were performed for compound **1** in both conformations in order to have experimental insight into the spatial structure of the molecule (Fig. 11). The thioamidic hydrogen, NH, was selectively excited and the NOE enhancements of other ^{1}H resonances were observed, discarding the data for the hydroxyl proton exchanging with residual water. Interatomic distances from NH were determined as linear regression slopes of the NOE buildups (Table 4). Since only relative ratios between individual distances are obtained from NOE buildups, a reference is needed. Our method was to minimize the sum of squares of differences between the experimental and DFT calculated distances between NH and hydrogens H6, and H6′ which are the nearest ones. We estimate the error in experimental distances in the order of 0.1 Å and it grows for larger distances.

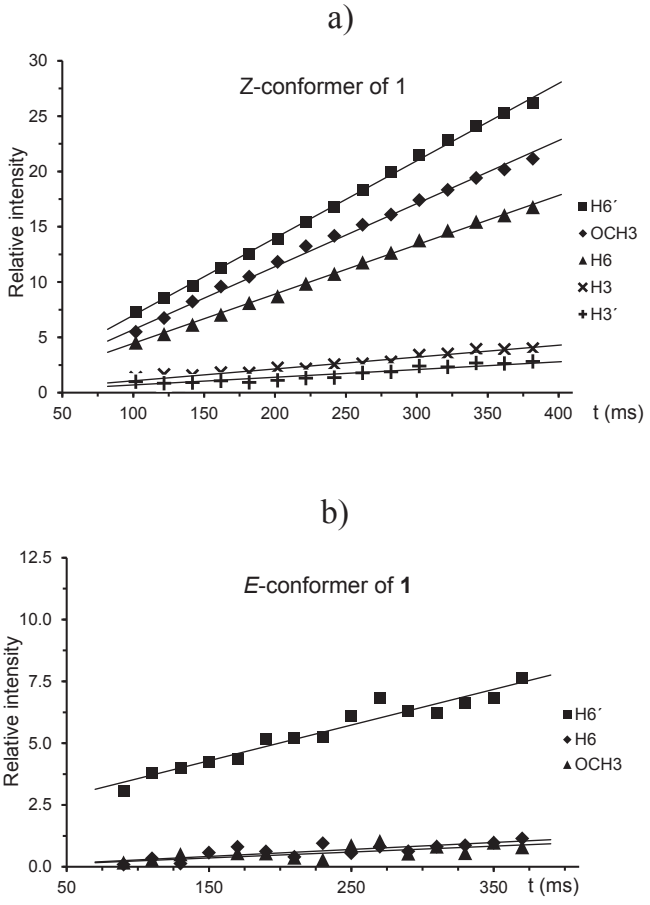

Fig. 11. NOE buildup curves while selectively exciting NH of **1** NH_Z a) or NH_E b). The NOE mixing time was systematically increased from 100 to 380 ms in 20 ms steps. All spectra were collected with 1024 transients for *Z* conformer and with 3000 for *E*. The recycling delay was set to 5 s (500 MHz, DMSO-d_6, 25 °C).

Table 4
Measured and calculated intramolecular distances in **1**

Distance (Å)				
	Z-conformer		*E*-conformer	
	1D NOE	calcd[a]	1D NOE	calcd[a]
NH–H6'	3.3	3.12	3.3	3.27
NH–H6	3.5	3.64	4.3	4.28
NH–H3'	4.8	5.05	N/A[b]	4.94
NH–H3	4.5	4.89	N/A[b]	6.24
NH–OCH_3	3.4	4.42	4.4	5.17
		4.59		5.63
		5.15		5.92

[a] Weighted average (ΔE_H) of values in Table 3.
[b] Data are not available due to too weak NOE enhancement to be measured; i.e., distance longer than 5 Å.

The intramolecular distances between various hydrogens of phenyl groups and the amide hydrogen vary by 0.5 Å among different structures (within the corresponding thioamide group conformation). This is more prominent in the case of H6 and H6′. However, the experimental values determined on the basis of the ^{1}H NMR spectra refer to the mean value of individual intramolecular distances. Therefore, for the comparison between the experiment and simulation (Table 4), the calculated mean values were obtained as averages weighted by ΔE_H. Inspection of Table 4 shows a very good agreement between experimental and theoretical distances: except for the methoxy group protons, the differences are few tenths of angstrom and the sequence matches perfectly. Distances from NH to the methoxy group hydrogens cannot be compared directly because of their free rotation along the CO bond which was not analyzed during the DFT calculations. In fact, it is evident from Fig. 10a, b that the motionally averaged position of CH_3 group must lie closer to the NH hydrogen which is in accordance with the experiment.

3. Conclusion

Based on the study of compound **1**, it was shown that the two series of NMR resonance signals of 2-methoxy-2′-hydroxythiobenzanilides are *E* and *Z*-conformers around the CS–NH bond. The more populated conformer is the *Z*-conformer (Fig. 5). By various chemical modifications, it was found that the sulfur atom of thioamide group and the steric properties of *ortho* substituents of the aromatic rings are responsible for the possibility to observe the two conformers. No intramolecular hydrogen bond is formed which would potentially stabilize the conformers.

From line-shape analysis of VT NMR spectra of compound **1**, it was revealed that the enthalpy change slightly favours the *E*-conformer over the *Z*-conformer by $\Delta H=(-3.1\pm1.3)$ kJ/mol. On the other hand, the entropy contribution $\Delta S=(-26.9\pm3.6)$ J/mol/K strongly prefers the *Z*-conformation. As a result, the *Z*-conformer dominates in a wide range of temperatures and the *Z*/*E* population ratio is 88:12 at 25 °C. These thermodynamic data are in agreement with the DFT/B3LYP/cpcm(DMSO) computational study of compound **1**. The energy difference between *Z* and *E*-conformer was found to be ΔE_H=4.1 kJ/mol, which can be compared to the experimental Gibbs free energy difference $\Delta G_{25\,^\circ C}=(+4.9\pm0.3)$ kJ/mol at 25 °C.

From the detailed analysis of VT NMR data of compound **1** it was also revealed that the energy of barrier of interconversion of the *Z*-conformer to the *E*-conformer $\Delta G^{\ddagger}_{25\,^{\circ}C}$=(+81.5±0.4) kJ/mol at 25 °C is described by activation enthalpy $\Delta H^{\dagger}$=(+77.7±1.7) kJ/mol and entropy $\Delta S^{\dagger}$=(−12.5±4.6) J/mol/K. The quantum-chemical calculated activation energy $\Delta E^{\ddagger}_{H}$=79.0 kJ/mol is quite similar to that obtained from the experiments. The high barrier is connected with the necessity of rotation along the NH–CS bond which is hindered by the conjugated system of p-orbitals rendering this bond partially double character.

Finally, computation analysis of rotation along the bonds connecting the phenyl groups with the thioamide moiety revealed more restricted motion in the *E*-conformer than in the *Z*-conformer. This can be explained by the entropy decrease observed experimentally in *E*-conformer. The computed rotational barriers about the Ar–CS and the Ar–NH bond of compound **1** indicate that this compound does not possess axial chirality. This finding is supported by missing splitting of resonance signal of methylene group in ^{1}H NMR spectra of compound **7** and **8**.

4. Experimental section

4.1. Materials

All of the chemicals and solvents used in this study were purchased from Sigma–Aldrich, Prague, Czech Republic and Penta, Prague, Czech Republic and were used without further purification. The reactions were monitored, and the purity of products was verified by thin layer chromatography in which the plates were coated with 0.2 mm of silica gel 60 F_{254} (Merck, Prague, Czech Republic) and visualized using UV irradiation (254 and 366 nm). Column chromatography was performed using silica gel 60 with a particle size of 0.063–0.2 mm (Fluka, Prague, Czech Republic).

4.2. General experimental procedures

The melting points were determined on a Melting Point M-560 apparatus (Bűchi Labortechnik AG, Flawil, Switzerland) in open capillaries and are uncorrected. The IR spectra were recorded on a Nicolet 6700 FTIR spectrometer (Thermo Fisher Scientific, Waltham, MA, USA) over the range of 400–4000 cm^{-1} using the single reflection ATR technique. ^{1}H NMR (500 MHz) and ^{13}C NMR (125.7 MHz) spectra were recorded on a Varian Inova VNMR S500 spectrometer. Chemical shifts were referenced to the residual solvent signal. Homonuclear ^{1}H–^{1}H connectivities were determined by gCOSY and NOESY with mixing time of 300–1200 ms. Heteronuclear ^{1}H–^{13}C connectivities were determined by phase-sensitive gHSQC NMR experiments, multiplicity-edited and optimized for a ^{1}J(H,C) of 146 Hz. Two- and three-bond ^{1}H–^{13}C connectivities were determined by gHMBC NMR experiments and optimized for a $^{2,3}J$(H,C) of 8 Hz and 5 Hz, respectively. If it is not stated otherwise, all of the NMR spectra were recorded at 25 °C in DMSO-d_6 solution. Elemental analysis (C, H, N, S) was performed on an automatic microanalyser CHNS-O CE instrument, FISONS EA 1110 (Thermo Fisher Scientific, Waltham, MA, USA).

4.3. NMR data analysis, fitting NMR spectra of compound 1

Line-shape analysis was performed on the ^{1}H NMR spectra of **1** measured at temperatures from 30.7 °C to 117.1 °C. The data were Fourier transformed using no apodization and manually phase corrected in MatNMR software package.[14] The least-square fits of the line-shape describing two-site asymmetrical chemical exchange to the experimental data were done by Asymexfit[15] toolbox (version 2.3) in MATLAB® environment (version R2009a). For each temperature, the fitting was done simultaneously for H3, H4, H6, H3′, H4′, H6′, and OCH3 resonances with a common equilibrium constant and exchange rate, together with residual water and DMSO peaks described as Lorentzian curves. The model assumed weakly coupled spins with equal scalar coupling constants for both *E* and *Z*-conformers, which allows calculation of the spectrum of a splitted peak as a sum of line-shapes for non-interacting resonances, shifted in frequency.[16] Zero-order phase correction and a linear baseline correction were added to the fitted parameters. Resonances of the NH and OH protons were excluded from the analysis because of their fast exchange.

To determine the exchange rates, the transverse relaxation times T_2^* (including the line broadening due to field inhomogeneity) of the exchanging sites need to be estimated for the case were no exchange is present, i.e., k_1=k_{-1}=0. However, the exchange modifies the line-shapes even for the lowest temperature measured, so the straightforward line-width approach cannot be reliably used. Instead, we followed the protocol based on Geyer et al.:[17] maximum possible rate k_1^{max} at 43.0 °C was estimated by repeated fitting for different fixed values of k_1. Other parameters (including chemical shifts, T_2^* and equilibrium constant) were optimized by the fitting procedure. Visual inspection of the results, comparison of chi-square values and rejection of too high relaxation times revealed that k_1^{max}=0.5 s^{-1}. Values of T_2^* obtained for k_1=0.2 s^{-1} were used in all further analysis as fixed parameters; values obtained for k_1^{min}=0.001 s^{-1} and k_1^{max}=0.5 s^{-1} were taken as confidence limits.

In spectra up to 55.3 °C, the exchange is slow, and two relatively narrow peaks can be distinguished for each pair of exchanging nuclei. Thus, chemical shifts of both conformers were optimized in the fit, along with the exchange parameters K=[*E*]/[*Z*]=k_1/k_{-1} and k_1. For temperatures from 61.5 °C up, severe broadening of the peaks of the *E* conformer occurs. This, together with overlap in the region of $H3_E$, $H3'_E$, and $H6'_E$, disables independent fitting of the chemical shifts of this conformer, δ_E. In this case, their values were fixed to linear extrapolations from temperatures at 55.3 °C and below. Prediction bands on 99% confidence level, calculated by OriginPro 9.0.0 were taken as confidence limits of δ_E.

Errors of the parameters optimized by the fits were estimated from repeated fits with varying the fixed values of T_2^* and δ_E within their confidence limits. Square roots of the sum of squares of 3σ of the parameter distributions obtained by these two methods are presented as uncertainties of the exchange parameters.

The temperature dependence of equilibrium constants K and rate constants k_1 obtained from the line-shape analysis were fitted by van't Hoff and Eyring equation, respectively, by Asymexfit[15] toolbox, using the inverse of experimental errors as weights in the chi-square calculation. The values of enthalpy and entropy are highly correlated, which is taken into consideration in estimating the error of the Gibbs free energy difference.

4.4. Quantum-chemical calculations

Quantum-chemical calculations were performed using the Gaussian 09 program suite,[18] revision A.02 (Gaussian, Inc.). Geometry optimization of each conformer of the studied molecule was done using following parameters: DFT method, B3LYP[19,20] hybrid functional, 6-311++G** basis set,[21] and the implicit solvent model COSMO[22,23] (cpcm) to mimic the DMSO environment. Models also included one explicit DMSO molecule H-bonded to the thioamide hydrogen for more precise simulation of solvent effects. All energy optimized structures were checked by the vibrational analysis. Possible starting conformations for the geometry optimization were generated based on the dihedral angle scan (5° step) of Ar–CS, Ar–NH, and CS–NH bonds using the same computational parameters as above with the exception of using a smaller basis set (6-31G).

Rotational barriers were calculated on the DFT/B3LYP/6-31G**/cpcm(DMSO) level. Each dihedral (torsion) angle was changed in

2.5° steps followed by the geometrical optimization. Scan was done both in clockwise and counterclockwise direction; the final energy profile was calculated as their minimum.

4.5. Synthetic part

General procedure for the preparation of acid chlorides (procedure A)

A substituted benzoic acid (6.0 mmol) was dissolved in $SOCl_2$ (20 mL), and refluxed under condenser equipped with a $CaCl_2$ drying tube for 3 h (see Fig. 12). Then, the excess of $SOCl_2$ was removed under reduced pressure, and the liquid residue was used without further purification for the preparation of benzamide.

General procedure for the preparation of benzamide (procedure B)

An appropriate benzoic acid chloride (6.0 mmol) was dissolved in ether (50 mL) and triethylamine (30.0 mmol) was added. Then, a solution of an appropriate aniline (6 mmol) in ether (100 mL) was added in one portion and the reaction mixture was stirred under a $CaCl_2$ drying tube at rt overnight (see Fig.12). Thereafter, the reaction mixture was extracted with a 5% solution of HCl (50 mL), with a 5% solution of $NaHCO_3$ (50 mL) and with water (50 mL). The organic phase was dried with Na_2SO_4 and purified using column chromatography and crystallization if necessary.

General procedure for the preparation of benzamide (procedure C)

First, an ether solution (100 mL) containing an appropriate benzoyl chloride (2.7 mmol) and an equimolar amount of TEA (2.7 mmol) was added drop wise at rt (1.5 h) into a stirred ether solution (40 mL) containing a substituted 2-aminophenol (2.7 mmol) (see Fig.12). After the addition, the mixture was stirred for 1 h at rt and then extracted with a 5% solution of HCl (50 mL), with a 5% solution of $NaHCO_3$ (50 mL) and with H_2O (50 mL). The organic phase was dried with Na_2SO_4 and purified using column chromatography and crystallization.

General procedure for the preparation of benzothioamide (procedure D)

A suspension of the starting benzamide (2.0 mmol) and an equimolar amount of P_4S_{10} (2.0 mmol) in pyridine (25 mL) was stirred and heated at reflux temperature until the starting benzamide was consumed (3–8 h). More P_4S_{10} was added if necessary (see Fig. 12). The unreacted P_4S_{10} was removed by the addition of ice water. The mixture was then extracted three times with chloroform (50 mL) and the organic phase was collected, dried with Na_2SO_4 and evaporated. The oil residue was purified by column chromatography on silica gel.

General procedure for the preparation of benzothioamide (procedure E)

To the benzanilide derivative (1.3 mmol) and P_4S_{10} (2.8 mmol) pyridine (10 mL) was added, and the reaction mixture was stirred at reflux temperature for 4 h. Then, $CHCl_3$ (40 mL), 5% aqueous solution of HCl (40 mL) and concentrated HCl (10 mL) were added, and the mixture was refluxed under vigorous stirring for 1 h (see Fig. 12). The organic phase was removed, and the aqueous phase was extracted three times with $CHCl_3$ (50 mL). Thereafter, the organic phases were collected, dried with Na_2SO_4 and evaporated. The oil residue was purified by column chromatography and crystallization.

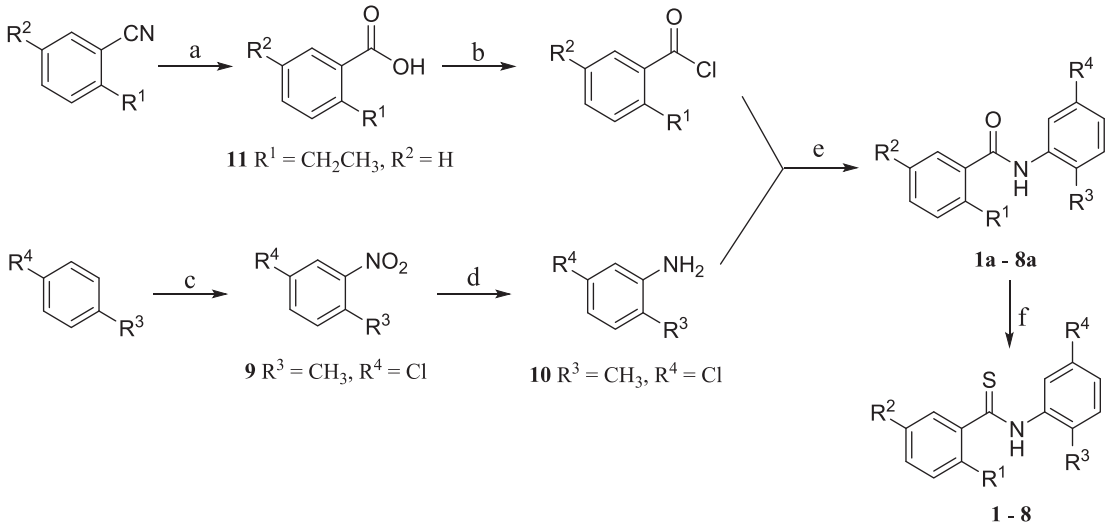

Fig. 12. General procedure for preparation of modification of compound **1**: R^1=H, OMe, Cl, Et; R^2=H, Cl; R^3=H, OH, Me, Et; R^4=H, Cl. Reagents: (a) 1. KOH, 2. HCl, (b) $SOCl_2$, (c) HNO_3, (d) Fe, AcOH, (e) TEA, (f) 1. P_4S_{10}, 2. HCl.

*4.5.1. 5-Chloro-N-(5-chloro-2-hydroxyphenyl)-2-methoxybenzamide (**1a**).*[24] The amide was prepared according to the procedure C. Yield: 71,8%, grey solid; mp: 232–234 °C; IR: 3296 (b, υ OH), 1648 (amide I), 1612, 1595 (υ CC aromatic), 1551 (amide II), 1498, 1483 (υ CC aromatic) cm^{-1}; ^1H NMR (DMSO-d_6, 500 MHz): δ 10.60 (1H, s, NH), 10.58 (1H, s, OH), 8.40 (1H, d, J=2.7 Hz, H6′), 7.98 (1H, d, J=2.8 Hz, H6), 7.62 (1H, dd, J=8.9 Hz, J=2.8 Hz, H4), 7.30 (1H, d, J=8.9 Hz, H3), 6.98 (1H, dd, J=8.5 Hz, J=2.7 Hz, H4′), 6.90 (1H, d, J=8.5 Hz, H3′), 4.03 (3H, s, OCH_3); ^{13}C NMR (DMSO-d_6, 125 MHz): δ 161.15, 156.19, 145.42, 133.31, 130.57, 128.13, 125.40, 123.50, 122.71, 122.66, 119.27, 115.73, 115.14, 57.19; Anal. Calcd for $C_{14}H_{11}Cl_2NO_3$ (312, 15) (%): C 53.87, H 3.55, N 4.49; Found: C 54.31, H 3.91, N 4.31.

*4.5.2. 5-Chloro-N-(5-chloro-2-hydroxyphenyl)-2-methoxybenzothioamide (**1**).* The thioamide was prepared according to the procedure E. Yield: 48.3%, yellow solid; mp: 147–149 °C, decomposition; IR: 3315 (b, υ OH), 1618, 1594, 1562, 1497, 1477, 1454 (υ CC aromatic) cm^{-1}. ^1H NMR (DMSO-d_6, 500 MHz): *Z*-conformer: δ 11.52 (1H, s, NH), 10.36 (1H, s, OH), 8.23 (1H, d, J=2.6 Hz, H6′), 7.76 (1H, d, J=2.8 Hz, H6), 7.48 (1H, dd, J=8.8 Hz, J=2.8 Hz, H4), 7.18 (1H, dd, J=8.7 Hz, J=2.6 Hz,

H4′), 7.16 (1H, d, *J*=8.8 Hz, H3), 6.96 (1H, d, *J*=8.7 Hz, H3′), 3.88 (3H, s, OCH_3); *E*-conformer: δ 11.61 (1H, s, NH), 10.10 (1H, s, OH), 7.30 (1H, d, *J*=2.8 Hz, H6), 7.23 (1H, dd, *J*=8.9 Hz, *J*=2.8 Hz, H4), 7.01 (1H, dd, *J*=8.7 Hz, *J*=2.7 Hz, H4′), 6.83 (1H, d, *J*=2.7 Hz, H6′), 6.76 (1H, d, *J*=8.9 Hz, H3), 6.72 (1H, d, *J*=8.7 Hz, H3′), 3.49 (3H, s, OCH_3). *Z*/*E* ratio 86:14. ^{13}C NMR (DMSO-d_6, 125 MHz): *Z*-conformer: δ 192.95, 153.49, 149.62, 132.46, 130.85, 130.67, 128.15, 127.30, 124.73, 124.22, 121.64, 117.29, 114.31, 56.66; *E*-conformer: δ 198.58, 151.41, 150.70, 132.81, 129.72, 129.04, 128.01, 128.04, 126.51, 123.62, 121.20, 117.24, 112.81, 55.50. Anal. Calcd for $C_{14}H_{11}Cl_2NO_2S$ (328.21) (%): C 51.23, H 3.38, N 4.27, S 9.77; Found: C 51.47, H 3.35, N 4.04, S 9.31.

*4.5.3. 3-Chloro-N-(5-chloro-2-hydroxyphenyl)benzamide (**2a**).*[25] The amide was prepared according to the procedure C. Yield: 61.8%, white solid; mp: 223–224 °C; IR: 3419 (υ NH), 3108 (b, υ OH), 1647 (amide I), 1608, 1591, 1566 (υ CC aromatic), 1537 (amide II), 1498 (υ CC aromatic) cm^{-1}; ^{1}H NMR (DMSO-d_6, 300 MHz): δ 10.08 (1H, s, NH), 9.68 (1H, s, OH), 8.00 (1H, t, *J*=1.9 Hz, H2), 7.95–7.87 (1H, m, H6), 7.74 (1H, d, *J*=2.6 Hz, H6′), 7.66 (1H, ddd, *J*=8.0 Hz, *J*=2.1 Hz, *J*=1.1 Hz, H4), 7.55 (1H, t, *J*=7.8 Hz, H5), 7.08 (1H, dd, *J*=8.7 Hz, *J*=2.6 Hz, H4′), 6.92 (1H, d, *J*=8.7 Hz, H3′); ^{13}C NMR (DMSO-d_6, 75 MHz): δ 164.21, 148.88, 136.41, 133.47, 131.76, 130.65, 127.70, 126.85, 126.55, 125.63, 124.26, 122.19, 117.17; Anal. Calcd for $C_{13}H_9Cl_2NO_2$ (282.12) (%): C 55.34, H 3.22, N 4.96; Found: C 55.24, H 3.42, N 4.85.

*4.5.4. 3-Chloro-N-(5-chloro-2-hydroxyphenyl)benzothioamide (**2**).* The thioamide was prepared according to the procedure E. Yield: 30.3%, yellow solid; mp: 124–125 °C, decomposition; IR: 3257 (υ NH), 3026 (b, υ OH), 1581, 1567, 1525, 1485, 1471 (υ CC aromatic) cm^{-1}. ^{1}H NMR (DMSO-d_6, 500 MHz): δ 11.37 (1H, s, NH), 10.05 (1H, s, OH), 7.91 (1H, t, *J*=1.9 Hz, H2), 7.88–7.80 (1H, m, H6), 7.64–7.57 (1H, m, H4), 7.53 (1H, d, *J*=2.7 Hz, H6′), 7.50 (1H, t, *J*=7.9 Hz, H5), 7.22 (1H, dd, *J*=8.8 Hz, *J*=2.7 Hz, H4′), 6.97 (1H, d, *J*=8.8 Hz, H3′). ^{13}C NMR (DMSO-d_6, 125 MHz): δ 196.88, 151.26, 143.21, 132.82, 130.72, 130.10, 128.26, 128.19, 127.76, 127.43, 126.55, 121.78, 117.92. Anal. Calcd for $C_{13}H_9Cl_2NOS$ (298.19) (%): C 52.36, H 3.04, N 4.70, S 10.75; Found: C 52.41, H 3.14, N 4.83, S 10.84.

*4.5.5. 5-Chloro-N-(3-chlorophenyl)-2-methoxybenzamide (**3a**).* The amide was prepared according to the procedure B. Yield: 71.7%, white solid; mp: 133–135 °C; IR: 3326 (υ NH), 3080 (υ CH aromatic), 1667 (amide I), 1588 (υ CC aromatic), 1525 (amide II), 1483, 1463 (υ CC aromatic) cm^{-1}; ^{1}H NMR (DMSO-d_6, 300 MHz): δ 10.35 (1H, s, NH), 7.91 (1H, t, *J*=2.1 Hz, H2′), 7.65–7.58 (2H, m, H6, H4′), 7.54 (1H, dd, *J*=8.8 Hz, *J*=2.8 Hz, H4), 7.36 (1H, t, *J*=8.1 Hz, H5′), 7.20 (1H, d, *J*=8.8 Hz, H3), 7.19–7.10 (1H, m, H6′), 3.87 (3H, s, OCH_3); ^{13}C NMR (DMSO-d_6, 75 MHz): δ 163.71, 155.47, 140.44, 133.26, 131.66, 130.61, 128.97, 126.76, 124.42, 123.62, 119.33, 118.32, 114.21, 56.50; Anal. Calcd for $C_{14}H_{11}Cl_2NO_2$ (296.15) (%): C 56.78, H 3.74, N 4.73; Found: C 56.41, H 3.64, N 4.66.

*4.5.6. 5-Chloro-N-(3-chlorophenyl)-2-methoxybenzotioamide (**3**).* The thioamide was prepared according to the procedure D. Yield: 11.2%, yellow solid; mp: 103–104 °C; IR: 3243 (υ NH), 1592, 1480, 1463 (υ CC aromatic) cm^{-1}; ^{1}H NMR ($CDCl_3$, 300 MHz): δ 10.55 (1H, s, NH), 8.42 (1H, d, *J*=2.7 Hz, H6), 7.86 (1H, t, *J*=2.0 Hz, H2′), 7.68–7.59 (1H, m, H4′), 7.38 (1H, dd, *J*=8.9 Hz, *J*=2.7 Hz, H4), 7.36 (1H, t, *J*=8.0 Hz, H5′), 7.28–7.23 (1H, m, H6′), 6.93 (1H, d, *J*=8.9 Hz, H3), 4.00 (3H, s, OCH_3); ^{13}C NMR ($CDCl_3$, 75 MHz): δ 193.31, 153.19, 140.10, 134.51, 134.41, 132.13, 129.86, 129.60, 126.95, 126.84, 124.06, 122.27, 113.08, 56.77; Anal. Calcd for $C_{14}H_{11}Cl_2NOS$ (312.21) (%): C 53.86, H 3.55, N 4.49, S 10.27; Found: C 53.54, H 3.27, N 4.65, S 10.35.

*4.5.7. 2,5-Dichloro-N-(5-chloro-2-hydroxyphenyl)benzamide (**4a**).* The amide was prepared according to the procedure C. Yield: 56.2%, white solid; mp: 212–213 °C; IR: 3381 (υ NH), 3159 (b, υ OH), 1655 (amide I), 1613, 1595 (υ CC aromatic), 1531 (amide II), 1464, (υ CC aromatic) cm^{-1}; ^{1}H NMR (DMSO-d_6, 500 MHz): δ 10.12 (1H, s, OH), 9.89 (1H, s, NH), 7.96 (1H, d, *J*=2.7 Hz, H6′), 7.73–7.65 (1H, m), 7.60–7.52 (2H, m), 7.05 (1H, dd, *J*=8.7 Hz, *J*=2.7 Hz, H4′), 6.90 (1H, d, *J*=8.7 Hz, H3′); ^{13}C NMR (DMSO-d_6, 125 MHz): δ 164.05, 147.74, 138.06, 131.80, 131.48, 131.01, 129.09, 129.05, 126.92, 125.08, 122.59, 122.21, 116.89; Anal. Calcd for $C_{13}H_8Cl_3NO_2$ (316.57) (%): C 49.32, H 2.55, N 4.42; Found: C 49.53, H 2.78, N 4.56.

*4.5.8. 2,5-Dichloro-N-(5-chloro-2-hydroxyphenyl)benzothioamide (**4**).* The thioamide was prepared according to the procedure E. Yield: 61.5%, yellow solid; mp: 152–153 °C, decomposition; IR: 3304 (υ NH), 3092 (b, υ OH), 1599, 1525, 1495, 1456 (υ CC aromatic) cm^{-1}. ^{1}H NMR (DMSO-d_6, 500 MHz): *Z*-conformer: δ 11.70 (1H, s, NH), 10.13 (1H, s, OH), 7.71 (1H, d, *J*=2.8 Hz, H6′), 7.62–7.40 (3H, m, H3, H4, H6), 7.21 (1H, dd, *J*=8.6 Hz, *J*=2.8 Hz, H4′), 6.97 (1H, d, *J*=8.6 Hz, H3′); *E*-conformer: δ 11.93 (1H, s, NH), 10.33 (1H, s, OH), 6.76 (1H, d, *J*=8.7 Hz), remaining signals overlapped by *Z* conformer. Z/E ratio 90:10. ^{13}C NMR (DMSO-d_6, 125 MHz): *Z*-conformer: δ 194.79, 150.87, 144.20, 131.57, 131.47, 129.72, 128.36, 128.17, 127.49, 127.18, 126.77, 121.71, 117.97; *E*-conformer: δ 197.50, 131.33, 131.10, 131.00, 130.75, 129.61, 128.79, 128.58, 127.24, 126.70, 126.33, 121.55, 117.58. Anal. Calcd for $C_{13}H_8Cl_3NOS$ (332.63) (%): C 46.94, H 2.42, N 4.21, S 9.64; Found: C 46.73, H 2.75, N 4.53, S 9.78.

*4.5.9. 4-Chloro-1-methyl-2-nitrobenzene (**9**).* H_2O (3.3 mL) was dispersed in 4-chlorotoluene (39.5 mmol) and whilst stirring the mixture of 65% HNO_3 (3.0 mL) and 96% H_2SO_4 (13.2 mL) was added drop wise at the temperature 50–55 °C. Then, the reaction mixture was stirred at 55 °C for 2 h, H_2O (50 mL) was added and the mixture was extracted three times with $CHCl_3$ (50 mL). The organic phases were collected, dried over Na_2SO_4 and purified by column chromatography.

Yield: 49.2%, yellow-white solid; mp: 37–38 °C; IR: 1556 (υ CC aromatic), 1521 (υ_{as} NO_2), 1481, 1451 (υ CC aromatic), 1347 (υ_s NO_2) cm^{-1}; ^{1}H NMR ($CDCl_3$, 300 MHz): δ 7.96 (1H, d, *J*=2.2 Hz, H3), 7.47 (1H, dd, *J*=8.2 Hz, *J*=2.2 Hz, H5), 7.29 (1H, d, *J*=8.2 Hz, H6), 2.57 (3H, s, CH_3); ^{13}C NMR ($CDCl_3$, 75 MHz): δ 149.35, 133.81, 133.01, 132.39, 132.02, 124.67, 19.95.

*4.5.10. 5-Chloro-2-methylaniline (**10**).* 4-Chloro-1-methyl-2-nitro benzene **9** (18.9 mmol) was dissolved in glacial acetic acid (50 mL) and H_2O (15 mL). The reaction mixture was stirred and heated to reflux. Iron powder (94.3 mmol) was added in portions over 15 min. After the addition of the iron powder, the mixture was refluxed for 30 min and then poured into ice-water (100 mL). The mixture was extracted three times with ethyl acetate (100 mL). Then, the organic phases were collected, extracted three times with a 5% solution of Na_2CO_3 (100 mL) and once with a saturated solution of NaCl (100 mL) before being dried with Na_2SO_4 and evaporated. The residue was purified by column chromatography.

Yield: 89.6%, white solid; mp: 24–25 °C; IR: 3385 (b, υ NH_2), 1622, 1576, 1494, 1448 (υ CC aromatic) cm^{-1}; ^{1}H NMR (DMSO-d_6, 300 MHz): δ 6.88 (1H, d, *J*=8.0 Hz, H3), 6.61 (1H, d, *J*=2.3 Hz, H6), 6.43 (1H, dd, *J*=8.0 Hz, *J*=2.3 Hz, H4), 5.11 (2H, br s, NH_2), 2.00 (3H, s, CH_3); ^{13}C NMR (DMSO-d_6, 75 MHz): δ 148.39, 131.32, 130.77, 120.03, 115.30, 113.02. 17.07.

*4.5.11. 5-Chloro-N-(5-chloro-2-methylphenyl)-2-methoxybenzamide (**5a**).* The amide was prepared according to the procedure B. Yield: 60.1%, white solid; mp: 198–200 °C; IR: 3341 (υ NH), 1663 (amide I), 1613, 1587 (υ CC aromatic), 1541 (amide II), 1480 (υ CC aromatic) cm^{-1}; ^{1}H NMR (DMSO-d_6, 500 MHz): δ 9.92 (1H, s, NH), 8.02 (1H, d, *J*=2.3 Hz, H6′), 7.84 (1H, d, *J*=2.9 Hz, H6), 7.61 (1H, dd, *J*=9.0 Hz, *J*=2.9 Hz, H4), 7.32–7.24 (2H, m, H3, H3′), 7.15 (1H, dd, *J*=8.1 Hz,

J=2.3 Hz, H4′), 3.99 (3H, s, OCH_3), 2.28 (3H, s, CH_3); ^{13}C NMR (DMSO-d_6, 125 MHz): δ 162.33, 155.99, 137.78, 132.65, 131.92, 130.37, 130.07, 128.50, 124.97, 124.47, 124.34, 122.31, 114.74, 56.98, 17.26, Anal. Calcd for $C_{15}H_{13}Cl_2NO_2$ (310, 18) (%): C 58.08, H 4.22, N 4.52; Found: C 58.25, H 4.39, N 4.38.

*4.5.12. 5-Chloro-N-(5-chloro-2-methylphenyl)-2-methoxybenzothioamide (**5**).* The thioamide was prepared according to the procedure D. Yield: 25.0%, yellow solid; mp: 142–144 °C; IR: 1597, 1577, 1530, 1486, 1463 (υ CC aromatic) cm^{-1}. ^1H NMR (DMSO-d_6, 500 MHz): *Z*-conformer: δ 11.58 (1H, s, NH), 7.54 (1H, d, J=2.7 Hz, H6), 7.46 (1H, dd, J=8.9 Hz, J=2.7 Hz, H4), 7.41 (1H, d, J=2.2 Hz, H6′), 7.35 (1H, d, J=8.3 Hz, H3′), 7.32 (1H, dd, J=8.3 Hz, J=2.2 Hz, H4′), 7.15 (1H, d, J=8.9 Hz, H3), 3.85 (3H, s, OCH_3), 2.25 (3H, s, CH_3); *E*-conformer: δ 12.04 (1H, s, NH), 7.49 (1H, d, J=2.7 Hz, H6), 7.27 (1H, dd, J=8.9 Hz, J=2.7 Hz, H4), 7.19 (1H, d, J=8.3 Hz, H3′), 7.10 (1H, dd, J=8.3 Hz, J=2.2 Hz, H4′), 6.79 (1H, d, J=2.2 Hz, H6′), 6.75 (1H, d, J=8.9 Hz, H3), 3.39 (3H, s, OCH_3), 2.27 (3H, s, CH_3). *Z*/*E* ratio 88:12. ^{13}C NMR (DMSO-d_6, 125 MHz): *Z*-conformer: δ 195.34, 153.10, 139.47, 133.83, 132.34, 130.23, 130.07, 129.28, 127.53, 127.15, 124.03, 113.91, 56.40, 17.18; *E*-conformer: δ 198.26, 151.24, 139.60, 132.33, 132.22, 131.68, 129.56, 129.43, 126.92, 126.11, 123.99, 112.98, 55.44, 17.28. Anal. Calcd for $C_{15}H_{13}Cl_2NOS$ (326.24) (%): C 55.22, H 4.02, N 4.29, S 9.83; Found: C 55.41, H 4.36, N 4.53, S 9.59.

*4.5.13. N-(2-Hydroxyphenyl)-2-methoxybenzamide (**6a**).*[26] The amide was prepared according to the procedure C. Yield: 73.2%, white solid; mp: 200–202 °C; IR: 3294 (υ NH), 3201 (b, υ OH), 1638 (amide I), 1614, 1598 (υ CC aromatic), 1555 (amide II), 1510, 1484, 1455 (υ CC aromatic) cm^{-1}; ^1H NMR (DMSO-d_6, 300 MHz): δ 10.57 (1H, s), 10.20 (1H, s), 8.37 (1H, d, J=7.9 Hz), 8.08 (1H, dd, J=7.8 Hz, J=1.8 Hz), 7.61–7.52 (1H, m), 7.25 (1H, d, J=8.3 Hz), 7.13 (1H, t, J=7.5 Hz), 6.95–6.89 (2H, m), 6.87–6.77 (1H, m), 4.03 (3H, s, OCH_3); ^{13}C NMR (DMSO-d_6, 75 MHz): δ 162.27, 157.35, 146.46, 133.66, 131.54, 127.43, 123.86, 121.58, 121.36, 119.92, 119.45, 114.76, 112.79, 56.63; Anal. Calcd for $C_{14}H_{13}NO_3$ (243.26) (%): C 69.12, H 5.39, N 5.76; Found: C 69.38, H 5.56, N 5.93.

*4.5.14. N-(2-Hydroxyphenyl)-2-methoxybenzothioamide (**6**).* The thioamide was prepared according to the procedure E. Yield: 46.7%, yellow oil; IR: 3289 (υ NH), 3046 (b, υ OH), 1585, 1537, 1515, 1489 (υ CC aromatic) cm^{-1}. ^1H NMR (DMSO-d_6, 500 MHz): *Z*-conformer: δ 11.39 (1H, s, NH), 9.97 (1H, s, OH), 8.28 (1H, dd, J=8.1 Hz, J=1.6 Hz, H6′), 7.88 (1H, dd, J=7.8 Hz, J=1.8 Hz, H6), 7.50–7.39 (1H, m, H4), 7.18–7.08 (2H, m, H3, H4′), 7.03 (1H, td, J=7.5 Hz, J=1.0 Hz, H5), 6.95 (1H, dd, J=8.2 Hz, J=1.4 Hz, H3′), 6.85 (1H, td, J=7.7 Hz, J=1.4 Hz, H5′), 3.89 (3H, s, OCH_3); *E*-conformer: δ 11.32 (1H, s, NH), 9.73 (1H, s, OH), 7.30 (1H, dd, J=7.6 Hz, J=1.8 Hz, H6), 7.16 (1H, overlapped by *Z*-conformer, H4), 6.99–6.93 (1H, m, H4′), 6.84 (1H, overlapped by *Z*-conformer, H5), 6.74 (1H, dd, J=8.1 Hz, J=1.3 Hz, H3′), 6.69 (1H, d, J=8.4 Hz, H3), 6.62 (1H, dd, J=8.3 Hz, J=1.6 Hz, H6′), 6.46 (1H, td, J=7.6 Hz, J=1.3 Hz, H5′), 3.43 (3H, s, OCH_3). *Z*/*E* ratio 88:12. ^{13}C NMR (DMSO-d_6, 125 MHz): *Z*-conformer: δ 193.98, 154.81, 150.42, 132.41, 131.87, 131.19, 127.83, 127.63, 125.11, 120.81, 118.91, 116.14, 112.47, 56.46; *E*-conformer: δ 199.89, 152.78, 151.30, 131.38, 130.09, 129.47, 127.85, 127.42, 126.26, 120.02, 118.19, 115.86, 111.00, 55.08. Anal. Calcd for $C_{14}H_{13}NO_2S$ (259.32) (%): C 64.84, H 5.05, N 5.40, S 12.36; Found: C 64.68, H 5.36, N 5.73, S 12.49.

*4.5.15. 2-Ethylbenzoic acid (**11**).*[27] 2-Ethylbenzonitrile (7.6 mmol) and KOH (24.8 mmol) were suspended in ethane-1,2-diol (10 mL) and stirred at 170 °C for 7 h. Then, the reaction mixture was cooled down to rt, H_2O (50 mL) was added and the resulting mixture was extracted three times with ether (30 mL). pH of the aqueous layer was adjusted to 1 by diluted HCl and the aqueous phase was extracted three times with ether (40 mL). Organic phases were collected, extracted three times with H_2O (40 mL) and dried over Na_2SO_4. The solvent was removed and obtained compound was directly used in the next step.[27]

Yield: 89.0%, white solid; mp: 64–65 °C; IR: 3400–2300 (b, υ OH), 2977 (υ_{as} CH_3), 2955 (υ_{as} CH_2), 2869 (υ_s CH_3), 1681 (υ CO), 1601, 1575, 1488, 1447 (υ CC aromatic) cm^{-1}; ^1H NMR (DMSO-d_6, 300 MHz): δ 12.79 (1H, br s, COOH), 7.76 (1H, d, J=7.0 Hz), 7.43 (1H, t, J=7.5 Hz), 7.33–7.21 (2H, m), 2.90 (2H, q, J=7.4 Hz, CH_2), 1.14 (3H, t, J=7.4 Hz, CH_3); ^{13}C NMR (DMSO-d_6, 75 MHz): δ 169.14, 145.12, 131.96, 130.54, 130.35, 130.34, 126.04, 27.03, 16.32.

*4.5.16. N-(5-Chloro-2-hydroxyphenyl)-2-ethylbenzamide (**7a**).* The amide was prepared according to the procedure C. Yield: 74.4%, white solid; mp: 151–152 °C; IR: 3379 (υ NH), 3155 (b, υ OH), 2972 (υ_{as} CH_3), 1650 (amide I), 1593 (υ CC aromatic), 1525 (amide II), 1493 (υ CC aromatic) cm^{-1}; ^1H NMR (DMSO-d_6, 300 MHz): δ 10.12 (1H, br s, OH), 9.36 (1H, s, NH), 7.89 (1H, d, J=2.7 Hz, H6′), 7.53–7.37 (2H, m), 7.37–7.24 (2H, m), 7.05 (1H, dd, J=8.6 Hz, J=2.7 Hz, H4′), 6.90 (1H, d, J=8.6 Hz, H3′), 2.76 (2H, q, J=7.5 Hz, CH_2), 1.18 (3H, t, J=7.5 Hz, CH_3); ^{13}C NMR (DMSO-d_6, 75 MHz): δ 168.32, 147.79, 141.99, 136.27, 130.24, 129.44, 127.45, 127.44, 125.93, 124.91, 122.62, 122.35, 117.05, 26.06, 16.09; Anal. Calcd for $C_{15}H_{14}ClNO_2$ (275, 73) (%): C 65.34, H 5.12, N 5.08; Found: C 65.57, H 4.92, N 5.38.

*4.5.17. N-(5-Chloro-2-hydroxyphenyl)-2-ethylbenzothioamide (**7**).* The thioamide was prepared according to the procedure E. Yield: 39.9%, Yellow-green solid; mp: 140–141 °C, decomposition; IR: 3351 (υ NH), 3144 (b, υ OH), 2962 (υ_{as} CH_3), 2930 (υ_{as} CH_2), 2870 (υ_s CH_3), 1603, 1530, 1499, 1487, 1453 (υ CC aromatic) cm^{-1}. ^1H NMR (DMSO-d_6, 500 MHz): *Z*-conformer: δ 11.32 (1H, s, NH), 10.12 (1H, s, OH), 7.56 (1H, d, J=2.7 Hz, H6′), 7.44–7.10 (5H, m, H3, H4, H5, H6, H4′), 6.95 (1H, d, J=8.7 Hz, H3′), 2.81 (2H, q, J=7.5 Hz, CH_2), 1.21 (3H, t, J=7.5 Hz, CH_3); *E*-conformer: δ 11.56 (1H, s, NH), 10.28 (1H, s, OH), 7.17–7.05 (5H, overlapped by *Z*-conformer, H3, H4, H5, H6, H4′), 6.75 (1H, d, J=8.7 Hz, H3′), 6.64 (1H, d, J=2.6 Hz, H6′), 3.18 (2H, q, J=7.6 Hz, CH_2), 1.07 (3H, t, J=7.6 Hz, CH_3). *Z*/*E* ratio 95:5. ^{13}C NMR (DMSO-d_6, 125 MHz): *Z*-conformer: δ 201.03, 151.24, 144.05, 139.09, 128.73, 128.67, 128.04, 127.78, 127.49, 126.90, 125.55, 121.69, 117.83, 25.41, 15.68; *E*-conformer: δ 203.12, 150.42, 141.13, 138.12, 130.65, 130.22, 128.42, 128.08, 127.79, 126.75, 125.16, 121.52, 117.34, 24.87, 14.72; Anal. Calcd for $C_{15}H_{14}ClNOS$ (291.80) (%): C 61.74, H 4.84, N 4.80, S 10.99; Found: C 61.57, H 4.95, N 4.58, S 11.21.

*4.5.18. 5-Chloro-N-(2-ethylphenyl)-2-methoxybenzamide (**8a**).* The amide was prepared according to the procedure B. Yield: 89.3%, white solid; mp: 114–116 °C; IR: 3341 (υ NH), 1663 (amide I), 1614, 1593 (υ CC aromatic), 1550 (amide II), 1485, 1474, 1456 (υ CC aromatic) cm^{-1}; ^1H NMR (DMSO-d_6, 300 MHz): δ 9.83 (1H, br s, NH), 7.90–7.79 (2H, m), 7.58 (1H, dd, J=8.9 Hz, J=2.9 Hz, H4), 7.33–7.22 (2H, m), 7.21 (1H, dd, J=7.8 Hz, J=1.8 Hz), 7.15 (1H, dd, J=7.3 Hz, J=1.5 Hz), 3.98 (3H, s, OCH_3), 2.65 (2H, q, J=7.6 Hz, CH_2), 1.18 (3H, t, J=7.6 Hz, CH_3); ^{13}C NMR (DMSO-d_6, 75 MHz): δ 162.37, 155.93, 136.11, 135.76, 132.34, 130.07, 128.83, 126.36, 125.48, 124.94, 124.76, 124.26, 114.62, 56.87, 24.22, 14.29; Anal. Calcd for $C_{16}H_{16}ClNO_2$ (289, 76) (%): C 66.32, H 5.57, N 4.83; Found: C 66.59, H 5.75, N 4.68.

*4.5.19. 5-Chloro-N-(2-ethylphenyl)-2-methoxybenzothioamide (**8**).* The thioamide was prepared according to the procedure D. Yield: 37.3%, Yellow solid; mp: 101–103 °C; IR: 3336 (υ NH), 2958 (υ_{as} CH_3), 2930 (υ_{as} CH_2), 2870 (υ_s CH_3), 1595, 1569, 1508, 1481, 1464, 1445 (υ CC aromatic) cm^{-1}. ^1H NMR (DMSO-d_6, 500 MHz): *Z*-conformer: δ 11.50 (1H, s, NH), 7.51 (1H, d, J=2.7 Hz, H6), 7.45 (1H, dd, J=8.8 Hz, J=2.7 Hz, H4), 7.37–7.25 (4H, m, H3′, H4′, H5′, H6′), 7.15 (1H, d, J=8.8 Hz, H3), 3.86 (3H, s, OCH_3), 2.64 (2H, q, J=7.5 Hz, CH_2), 1.17 (3H, t, J=7.5 Hz, CH_3); *E*-conformer: δ 11.98 (1H, s, NH), 7.38 (1H, d, J=2.8 Hz, H6), 7.24–7.22 (1H, m, H4), 7.24–7.15 (1H, m),

7.09 (1H, dd, *J*=7.6 Hz, *J*=1.4 Hz), 6.91 (1H, td, *J*=7.7 Hz, *J*=1.5 Hz), 6.76 (1H, dd, *J*=7.3 Hz, *J*=1.3 Hz), 6.72 (1H, d, *J*=9.1 Hz, H3), 3.39 (3H, s, OCH_3), 2.49 (2H, q, *J*=7.5 Hz, CH_2) 1.23 (3H, t, *J*=7.5 Hz, CH_3). *Z*/*E* ratio 95:5. ^{13}C NMR (DMSO-d_6, 125 MHz): *Z*-conformer: δ 195.44, 153.07, 140.54, 137.87, 134.15, 130.01, 129.23, 129.17, 128.01, 127.96, 126.45, 123.97, 113.88, 56.35, 24.27, 15.05; *E*-conformer: 198.01, 151.51, 138.64, 137.79, 132.72, 130.39, 129.68, 129.09, 127.78, 127.52, 125.62, 123.80, 113.01, 55.52, 23.19, 13.51; Anal. Calcd for $C_{16}H_{16}ClNOS$ (305.82) (%): C 62.84, H 5.27, N 4.58, S 10.48; Found: C 62.89, H 5.45, N 4.77, S 10.59.

Acknowledgements

This work was supported by the Research project IGA NT 13346 (2012) and by the Charles University in Prague (SVV 260 183).

Supplementary data

Supplementary data associated with this article can be found in the online version, at http://dx.doi.org/10.1016/j.tet.2016.02.035.

References and notes

1. Chabaud, L.; Clayden, J.; Helliwell, M.; Page, A.; Raftery, J.; Vallverdu, L. *Tetrahedron* **2010**, *66*, 6936–6957.
2. Curran, D. P.; Hale, G. R.; Geib, S. J.; Balog, A.; Cass, Q. B.; Degani, A. L. G.; Hernandes, M. Z.; Freitas, L. C. G. *Tetrahedron: Asymmetry* **1997**, *8*, 3955–3975.
3. Bowles, P.; Clayden, J.; Tomkinson, M. *Tetrahedron Lett.* **1995**, *36*, 9219–9222.
4. Clayden, J.; Westlund, N.; Wilson, F. X. *Tetrahedron Lett.* **1996**, *37*, 5577–5580.
5. Clayden, J.; Pink, J. H. *Tetrahedron Lett.* **1997**, *38*, 2561–2564.
6. Clayden, J.; Darbyshire, M.; Pink, J. H.; Westlund, N. *Tetrahedron Lett.* **1997**, *38*, 8587–8590.
7. Clayden, J.; Vallverdu, L.; Helliwell, M. *Chem. Commun.* **2007**, 2357–2359.
8. Clayden, J.; Lund, A.; Vallverdu, L.; Helliwell, M. *Nature* **2004**, *431*, 966–971.
9. Clayden, J.; Johnson, P.; Pink, J. H.; Helliwell, M. *J. Org. Chem.* **2000**, *65*, 7033–7040.
10. Dantale, S.; Reboul, V.; Metzner, P.; Philouze, C. *Chem.—Eur. J.* **2002**, *8*, 632–640.
11. Ach, D.; Reboul, V.; Metzner, P. *Eur. J. Org. Chem.* **2003**, *2003*, 3398–3406.
12. Ach, D.; Reboul, V.; Metzner, P. *Eur. J. Org. Chem.* **2002**, *2002*, 2573–2586.
13. Kozic, J.; Novotna, E.; Volkova, M.; Stolarikova, J.; Trejtnar, F.; Wsol, V.; Vinsova, J. *Eur. J. Med. Chem.* **2012**, *56*, 108–119.
14. van Beek, J. D. *J. Magn. Reson.* **2007**, *187*, 19–26.
15. Římal, V.; Štěpánková, H.; Štěpánek, J. *Concepts Magn. Reson. Part A* **2011**, *38A*, 117–127.
16. Hansen, D. F.; Led, J. J. *J. Magn. Reson.* **2003**, *163*, 215–227.
17. Geyer, M.; Schweins, T.; Herrmann, C.; Prisner, T.; Wittinghofer, A.; Kalbitzer, H. R. *Biochemistry* **1996**, *35*, 10308–10320.
18. Frisch, M. J.; Trucks, G. W.; Schlegel, H. B.; Scuseria, G. E.; Robb, M. A.; Cheeseman, J. R.; Scalmani, G.; Barone, V.; Mennucci, B.; Petersson, G. A.; Nakatsuji, H.; Caricato, M.; Li, X.; Hratchian, H. P.; Izmaylov, A. F.; Bloino, J.; Zheng, G.; Sonnenberg, J. L.; Hada, M.; Ehara, M.; Toyota, K.; Fukuda, R.; Hasegawa, J.; Ishida, M.; Nakajima, T.; Honda, Y.; Kitao, O.; Nakai, H.; Vreven, T.; Montgomery, J., J. A.; Peralta, J. E.; Ogliaro, F.; Bearpark, M.; Heyd, J. J.; Brothers, E.; Kudin, K. N.; Staroverov, V. N.; Kobayashi, R.; Normand, J.; Raghavachari, K.; Rendell, A.; Burant, J. C.; Iyengar, S. S.; Tomasi, J.; Cossi, M.; Rega, N.; Millam, J. M.; Klene, M.; Knox, J. E.; Cross, J. B.; Bakken, V.; Adamo, C.; Jaramillo, J.; Gomperts, R.; Stratmann, R. E.; Yazyev, O.; Austin, A. J.; Cammi, R.; Pomelli, C.; Ochterski, J. W.; Martin, R. L.; Morokuma, K.; Zakrzewski, V. G.; Voth, G. A.; Salvador, P.; Dannenberg, J. J.; Dapprich, S.; Daniels, A. D.; Farkas, O.; Foresman, J. B.; Ortiz, J. V.; Cioslowski, J.; Fox, D. J. *Gaussian 09, Revision A02*; Gaussian: Wallingford, CT, 2009.
19. Kim, K.; Jordan, K. D. *J. Phys. Chem.* **1994**, *98*, 10089–10094.
20. Stephens, P. J.; Devlin, F. J.; Chabalowski, C. F.; Frisch, M. J. *J. Phys. Chem.* **1994**, *98*, 11623–11627.
21. Ditchfield, R.; Hehre, W. J.; Pople, J. A. *J. Chem. Phys.* **1971**, *54*, 724–728.
22. Klamt, A.; Schuurman, G. *J. Chem. Soc., Perkin Trans. 2* **1993**, 799–805.
23. Klamt, A. Cosmo and Cosmo-Rs In*Schleyer, P. R., Allinger, N. L., Clark, T., Gasteiger, J., Kollman, P. A., Schaefer, H. F., III, Schreiner, P. R., Eds.. Encyclopedia of Computational Chemistry*; John Wiley & Sons: Chichester, U.K, 1998; 1, pp 604–615.
24. Biagi, G.; Giorgi, I.; Livi, O.; Nardi, A.; Calderone, V.; Martelli, A.; Martinotti, E.; Salerni, O. L. *Eur. J. Med. Chem.* **2004**, *39*, 491–498.
25. Calderone, V.; Coi, A.; Fiamingo, F. L.; Giorgi, I.; Leonardi, M.; Livi, O.; Martelli, A.; Martinotti, E. *Eur. J. Med. Chem.* **2006**, *41*, 1421–1429.
26. Shibasaki, Y.; Toyokawa, F.; Ando, S.; Ueda, M. *Polym. J.* **2007**, *39*, 81–89.
27. Reimann, E.; Erdle, W.; Weigl, C.; Polborn, K. *Monatsh. für Chem.* **1999**, *130*, 313–326.